Review of Scientific Instruments, **68** (4), 1759 (1997).

A Versatile, Stable Scanning Proximal Probe Microscope

C.L. Jahncke* and H.D. Hallen
North Carolina State University, Physics Department, Raleigh, NC 27608
*Present address: St. Lawrence University, Physics Department, Canton, NY 13617

We present a novel scanning proximal probe microscope design utilizing a piezo-electric driven coarse positioning mechanism in x, y, and z, while maintaining relatively small lateral dimensions. The instrument is suitable for insertion into a dewar. The primary purpose of this work is to develop a stable yet versatile instrument in order to meet the signal averaging limitations imposed by low signal level measurements. We have implemented a near field scanning optical microscope (NSOM) with this system, whose key features include simultaneous detection of reflected and transmitted signals, unique 'center of mass' tip oscillator for shear force feedback, and overall microscope stability.

I. Introduction

The family of scanned probe microscopes (SPM) [1] includes the scanning tunneling microscope (STM) [2], the atomic force microscope (AFM) [3], the scanning Hall probe microscope (SHPM) [4, 5], the near-field scanning optical microscope (NSOM) [6, 7], and related techniques. These instruments are all very similar to each other, differing mainly in the probe which is placed in close proximity to the sample. In this paper, we discuss the instrument and neglect many of the details about which physical quantities are detected by the probe. We will, however, mention some of the instrumentation issues relevant to AFM and NSOM signal collection. Some specific commonalities of the microscopes mentioned above include: 1) the ability to scan a probe relative to a sample with sub-nanometer precision while using a feedback scheme to fix the probe-sample distance, 2) the ability to transfer that probe from sample loading distances (~0.1-few mm) to the proximity of the sample surface (~0.1-several nm), and 3) a degree of thermal and vibrational stability. All benefit from additional capabilities such as coarse lateral positioning on a mm or larger scale with micron or finer resolution, and from the versatility to operate over a range of temperatures or in a variety of environments, such as in solution or in vacuum in addition to ambient. These additional design constraints affect the best choice of the mechanical design due to size and coupling (mainly of the coarse motion mechanisms) to the external world. The differences in the instruments, besides the probes, relate to the different resolutions obtainable and the sample information desired. Both affect the scan size which is used and the required instrument stability. Another factor which depends upon the particular sample or measurement rather than the probe is the averaging time. It can be very long with imaging time exceeding 10 hours for NSOM imaging of Raman scattered light [8] or SHPM imaging of weak, anisotropic vortices in superconductors [9]. Alternatively, imaging time can and must proceed at close to video rates for studies of high temperature surfaces with an STM [10].

In this paper, we will highlight some of the novel features of a microscope which can perform most of these tasks quite well. Our approach is to design for the most demanding application, leaving flexibility when possible. In particular, we focus on stability for signal averaging, lateral size for insertion into a dewar or small space, and optical access for a variety of purposes. An overview of the instrument is presented first. Then we will explore several features of our design which are unique and contribute to the versatility and/or stability of our instrument beginning with general probe applicability, moving to AFM/NSOM applicability and ending with NSOM specific information. Data will be presented which demonstrates each of the microscope's assets.

II. Microscope Overview

We begin by giving an overview of the operation of the instrument highlighting the features which contribute to its stability. There are several concepts that must be considered in order for the microscope to be both stable and flexible. Those which contribute primarily to stability include the

following: (1) thermal fluctuations, (2) rigidity, and (3) mechanical loop (4) physical size and (5) sample mounting. A schematic of the microscope is shown in figure 1 and a photograph in figure 2. The design is compact with overall dimensions of 1 3/4" x 1 3/4" x 4". The microscope is machined primarily out of titanium (which has a thermal expansion which is close to that of the PZT-4 piezoelectric ceramic over a wide temperature range). Thermal drift is reduced by using copper in limited quantities to compensate for the thermal expansion of the titanium and piezoelectric materials, primarily in the z-direction. Since it has about twice the expansion coefficient of these other materials over a wide temperature range, the copper may be used to compensate for empty space in the mechanical loop. The entire instrument is placed in a thermally insulated copper chamber to limit thermal fluctuations. In this situation, we found the lateral drift to be 200 nm over the duration of a 10 hour scan or ~ 0.3 nm/min.[8] In the lateral dimension, the small size and the thermal isolation are the primary factors in the thermal drift. The drift in the z direction was 30 nm in ten hours or ~ 0.05 nm/min. The microscope can also be placed into a dewar for low temperature experiments. The coarse positioning of the tip to the sample is accomplished with an all electronic inertial slip stick motion (described in detail below), eliminating the need for stepper motors or other mechanical devices.

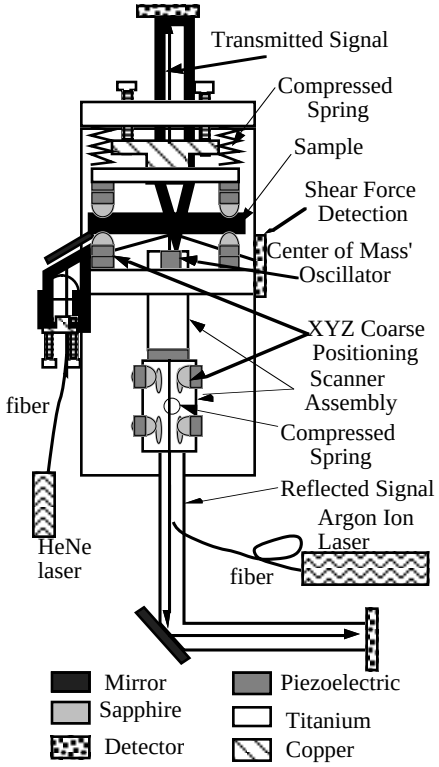

Figure 1. Schematic of the microscope highlighting some of its novel features.

A specific feature of the instrument used for NSOM or lateral force microscopy includes the use of conventional shear force feedback[11, 12] to maintain the tip to sample distance. Shear force feedback involves monitoring the amplitude of the fiber probe as it is oscillated at it's resonance frequency in along the sample surface. The design implemented here is unusual in that the feedback and scanning components are all on the same side of the sample. The sample remains fixed except during coarse lateral positioning. This is accomplished with a novel center-of-mass probe oscillator described below which takes advantage of the fact that the tip is at the end of the scan piezo. Scanning the probe is convenient when large samples are to be studied, as the microscope can be placed directly on the sample. This geometry can be used with recent non-optical probe amplitude detection schemes [13-15], but we have implemented the optical lever arm method. This feedback method is typically implemented by focusing a laser onto the oscillating fiber probe and then bouncing this signal off of the sample and onto a photodiode. The diffraction pattern from the probe moves across the photodiode generating the feedback signal. A reflective sample produces a large signal, but a transparent sample will still have some Fresnel reflectivity and may be used as well. In our design, the shear force feedback signal is generated by illuminating the tip with a fiber and lens-mirror assembly and the signal is detected with a photo-diode all of which are rigidly attached to the microscope (see figure 1) resulting in a small mechanical loop and reducing susceptibility to vibrations. In addition this allows for easy placement into a vacuum or dewar -- requiring only fiber coupling.

With flexibility in mind, this microscope is designed to be easily converted to operate in several different configurations and in different environments. The transition between an STM and an NSOM is simple, merely requiring a change in probe. With the removal of an extender block, a shorter tube scanner can be used which will have a smaller expansion per volt and, therefore, more sensitive measurements can be made. To change into a conventional AFM would require more substantial modifications, however, shear force measurements can be easily obtained. The microscope is capable of simultaneous detection of transmitted and reflected light from the sample and, therefore, can accommodate both transparent and opaque samples for NSOM operation. In

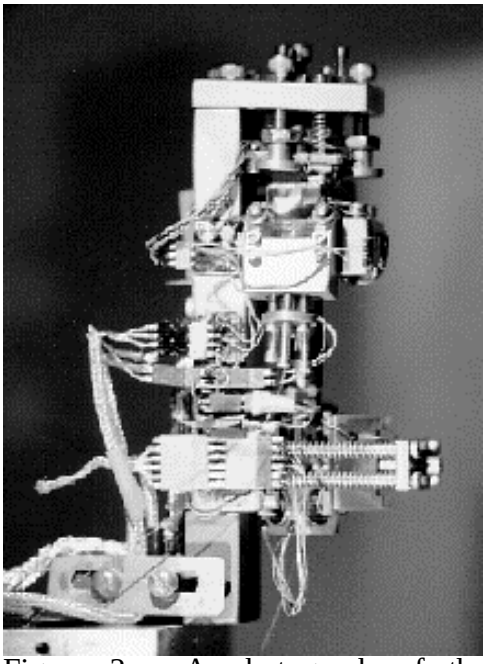

Figure 2. A photograph of the instrument from a view looking at the left in figure 1.

addition, the choice of materials and assembly make the instrument cryogenically compatible. Sample mounting is simple and can be accomplished in vacuum with a wobble stick.

The resulting monolithic instrument is small, stable and easily moved into different environments. In the remainder of the paper we will discuss the implementation of the all-electronic coarse positioning system, the center of mass probe oscillator, and finally the ability to collect light along both axial directions simultaneously.

III. Coarse Positioning

In this microscope design the probe is scanned rather than the sample. The scanner assembly is a plug-in module which can be removed to facilitate the ease of changing probes. An all electronic coarse motion system is employed to position the probe axially and the sample laterally. The positioning can be operated against, with , or normal to gravitational forces. We use an inertial slip/stick approach to accomplish motion. Shear piezos (1/8" x 3/16" x 1/16") provide the mechanism for instigating movement. Sapphire hemispheres epoxied to the shear piezos slide on sapphire plates for z-motion giving a low coefficient of friction as well as a hard flat surface to move across. There are eight hemisphere/pad contacts. Four of these are rigidly mounted to the frame and restrict lateral motion along and rotation about the x and y axes. The other four on a spring-mounted block restrict the block's motion and insure the scanner/slider is held against all the hemispheres. The scanner is free to move in z, and the rotation about z is minimized. For x and y motion, the sapphire hemispheres slide on the sample (or sample holder). A compressed spring is used to (evenly) adjust the frictional force between the sapphire balls and plates for both the x-y motion and the z motion as seen in figures 1 and 2. Note that the sliders are supported solely by the hemispheres and that they all move at once to produce motion. Figure 1 shows the sapphire hemispheres and shear piezos used for coarse positioning.

For the slip/stick type of motion, a spiked voltage pulse to a piezo induces sliding. It is important that the waveform has a sharp change in acceleration in order to induce motion. In addition, according to Ch. Renner et. al. [16], there is one acceleration condition required to move in the direction of gravity and another condition to move against gravity; a cycloid waveform is recommended. In our instrument, the cusp wave form shown in figure 3 is used. This signal is generated by putting a ramp function through a nonlinear amplifier consisting of an op-amp, two diodes, and a variable resistor also shown in figure 3. This has the advantages of being very simple and inexpensive as well as effective. This signal passes through a high voltage amplifier so that the piezos experience +/-150 volts for each step. Reversing the polarity of the signal changes the direction of motion. The frequency used for the steps is approximately 2 kHz. The number of steps is controlled by sending pulses from the computer into the trigger input on a function generator. The

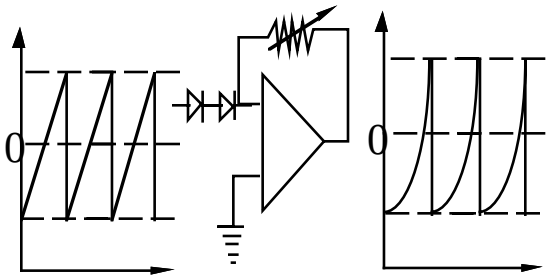

Figure 3. A simple circuit to generate the sharp waveforms necessary for producing slip-stick motion is shown. A ramp waveform from a function generator triggered by a computer passes through a nonlinear amplifier circuit (consisting of two diodes, an op-amp and a variable resistor) and is then passed through a high voltage amplifier (not shown) before being applied to the piezo's to generate the slip stick coarse motion.

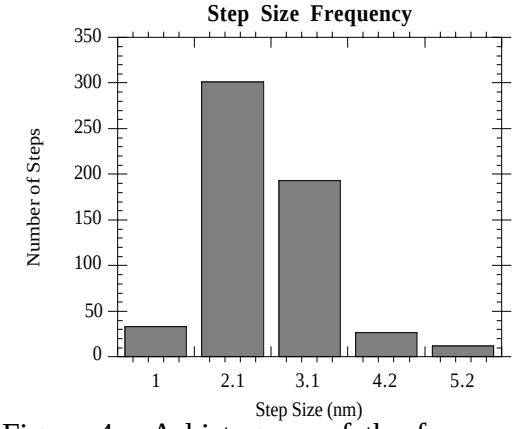

Figure 4. A histogram of the frequency of the step size for several hundred steps.

distance the tip assembly can travel is only limited by the size of the sapphire plates which are 1/4" in diameter.

There is a step size dependence on the frictional force imposed by the spring. Thus, the spring force is critical. If the spring force is too low or too high, no motion can be achieved. A low spring force results in longer steps. However, for a given spring force, the step size is nominally constant as can be seen in figure 4. The step size is determined by taking single steps while in feedback and monitoring the corresponding change in feedback voltage to the z-piezo. Recording this z voltage change for several hundred single steps during several different sample approaches, results in the histogram shown in figure 4. Using this method, we have obtained typical step sizes of 2-3 nm.

IV. Center-of-Mass Oscillator

The mechanism we use for generating the oscillating motion of the tip for shear force feedback is based on center of mass (CM) principles. Plate piezos (1/16" x 1/8" x 1/8") are glued to both sides of the end of the tube scanner assembly (described below) using a conducting silver epoxy. Voltages are applied so that one piezo contracts while the other expands. This causes an oscillatory change in the piezo mass distribution, see figure 5.

The lateral resonant frequency of the piezo scanning tube and extender is much lower than the typical 10's of kHz required to drive the probe at resonance. Thus, *at these frequencies*, the end of the extender tube, probe, lens, and plate piezos act like a freely floating body--the center of mass must remain fixed. Since the plate piezo mass distribution changes, the probe etc.. must move in order to compensate just as your head moves as you move your arms in the same direction in and out from your body. The amplitude of the fiber motion, ΔL_{fiber}, depends on the amplitude of the plate piezo motion, ΔL_{piezo}, as well as on the mass of the lens, the mass of the plate piezos, the mass of the fiber holder and fiber and the mass of the displaced titanium leading to the equation

$$\Delta L_{fiber} = \Delta L_{piezo} \frac{m_{platepiezo}}{\text{total mass}} \qquad (1)$$

The tip of the fiber will oscillate at an amplitude $\approx Q \times (\Delta L_{fiber})$ at resonance. This corresponds to a tip displacement of 3 nm for a fiber with a Q = 100 for lateral vibration and a 1 V oscillation voltage for our particular instrument. This method of producing the tip oscillation is compact and

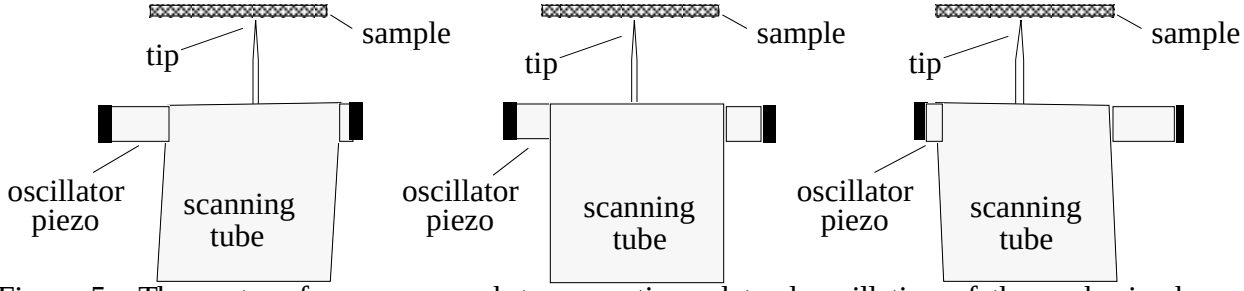

Figure 5. The center of mass approach to generating a lateral oscillation of the probe is shown schematically at a few points of the motion. As the oscillator piezos change their mass distribution, the probe and other mass at the end of the scan tube must move to compensate since the combination freely moves in the lateral dimension at the driven frequency.

effective. It takes advantage of components that are already present in conjunction with only minor additions. The method has two advantages over the use of a single plate piezo. First, the plate piezo's are mounted on the outer edge of the tube assembly so that they do not block any of the light for operation in a reflection mode. Second, the use of a tip glued to a single piezo at the end of the scanner piezo would still result in a center of mass type motion, but it would complicate the knowledge of the absolute tip motion. In figure 6 we show a tip resonance generated by our oscillator. The topographical image in figure 7a was obtained using our CM oscillator.

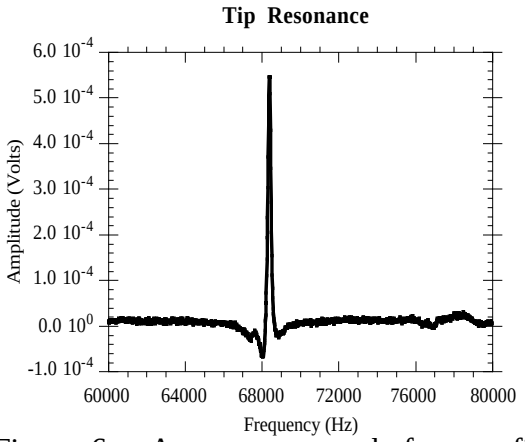

Figure 6. A resonance peak from a fiber optic probe tip is shown where the resonance frequency is 68.4 kHz and the Q is 380. The resonance is driven by the center of mass oscillator described above, and the tip oscillation detected by an optical lever arm method.

V. Reflection/Transmission NSOM

When operating an NSOM, there are a number of occasions where it may be desirable to study either the reflected or the transmitted light from a sample of interest. Rather than build two separate microscopes, we have one microscope which will perform either function or both simultaneously. The NSOM tapered aluminum-coated fiber optic probe is scanned across the sample using a tube scanner (1/4" diameter, 1" long, 0.02" wall thickness) with a 1" titanium extender to increase the scan range to 25 µm. The increase in scan range by the addition of an extender is analogous to bending your wrist while you hold a ruler in your hand verses bending your arm. This geometry seems to reduce distortion compared to the use of a larger piezo tube, since the lateral motion produced bending the piezo along its length contains more distortion than that produced by using the angle at the end of a shorter active element. Into the end of the titanium extender, a glass aspheric lens [Corning] with a numerical aperture of 0.55 is epoxied. A hole is diamond-drilled into the center of the lens into which a short section of hypodermic tubing is epoxied. The fiber is super-glued into the tube with its tip at the focal point of the lens in order to collect the reflected light from the sample. This geometry has advantages over light collection from the side for several reasons. When collecting the light from the side it is possible for sample features to block some of the light from reaching the lens. This shadowing can be a significant problem if the sample has coarse features. This geometry also allows for more freedom in sample mounting and manipulation. The transmitted light is collected with a similar asphere positioned so that the sample surface is at the focal point. In this way both the reflected and transmitted light can be collected simultaneously. Either can easily be directed into a detector or a spectrometer.

In figure 7 we show three 3 µm x 3 µm images obtained simultaneously. The sample is Rb doped KTP. The Rb doped regions are elevated 12 nm above the KTP surface due to the induced stress. This can be observed in the lateral force topography image shown in figure 7a where the upper right hand corner is a Rb doped region. The Rb changes the refractive index of the material so that the RTP region has an index 0.027 higher than the KTP. This results in optical contrast in addition to the topographical contrast as can be seen in figure 7b and 7c. Figure 7b is the transmission image and figure 7c is the reflection image.

VI. Conclusions

In conclusion we have developed a novel scanning probe microscope which is very stable and capable of operating in a variety of environments. The most notable features of this instrument include an all electronic coarse positioning system applicable to any scanned probe microscope, a CM oscillator to drive a probe at resonance, the ability to simultaneously collect both transmitted and reflected optical signals for NSOM, and overall stability.

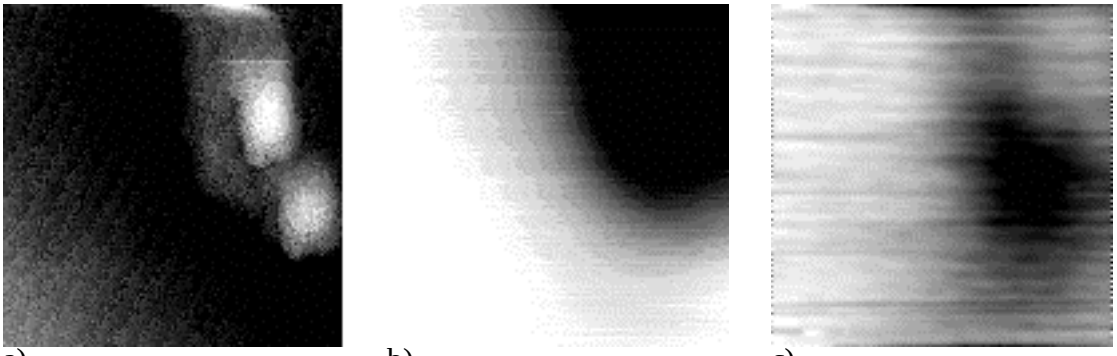

a) b) c)

Figure 7. Three simultaneously obtained 3 μm x3 μm images of a Rb doped KTP sample. a) shows the sample topography, b) is a transmission image and c) is a reflection image.

VII. Acknowledgments

We would like to thank Dr. Mark Roelofs of the Dupont Company for the Rb doped KTP samples used in this study. This work was supported by the U.S. Army Research Office through grants DAAHO4-94-G-0156 and DAAH04-93-G-0194.

REFERENCES

[1] J.A. Stroscio and William J. Kaiser, (Academic Press, Boston 1993)
[2] G. Binnig, H. Rohrer, Ch. Gerber and E. Weibel, Physical Review Letters **49**, 57 (1982).
[3] G. Binnig and C.F. Quate, Physical review Letters **56**, 930 (1986).
[4] H.D. Hallen, R. Seshadri, A.M. Chang, R. Miller, L.N. Pfeiffer, K. West, C.A. Murray and H. F. Hess, Phys. Rev. Lett. **71**, 3007 (1993).
[5] A.M. Chang, H.D. Hallen, H.F. Hess, H.L. Kao, J. Kwo, R. Wolf, J. van der Zeil and T.Y. Chang, Appl. Phys. Lett. **61**, 1974 (1992).
[6] D.W. Pohl, W. Denk and M. Lanz, Applied Physics Letters **44**, 651 (1984).
[7] M.A. Paesler and P.J. Moyer, "Near-Field Optics: Theory, Instrumentation and Applications," (John Wiley and Sons, Inc., New York, 1996).
[8] C.L. Jahncke, M.A. Paesler and H.D. Hallen, Appl. Phys. Lett. **67**, 2483 (1995).
[9] A.M. Chang, H.D. Hallen, H.F. Hess, H.L. Kao, J. Kwo, A. Sudbø and T.Y. Chang, Europhys. Lett. **20**, 645 (1992).
[10] A. Feltz, U. Memmert and R.J. Behm, Chemical Physics Letters **192**, 271 (1992).
[11] E. Betzig, P.L. Finn and J.S. Weiner, Applied Physics Letters **60**, 2484 (1992).
[12] R. Toledo-Crow, P. C. Yang, Y. Chen and M. Vaez-Iravani, Applied Physics Letters **60**, 2957 (1992).
[13] Khaled Karrai and Robert D. Grober, Applied Physics Letters **66**, 1842 (1995).
[14] J.W.P. Hsu, M. Lee and B.S. Deaver, Review of Scientific Instruments **66**, 3177 (1995).
[15] Mark Lee, E.B. McDaniel and J.W.P. Hsu, Review of Scientific Instruments **67**, 1468 (1996).
[16] Ch. Renner, Ph. Niedermann, A.D. Kent and O Fischer, Review of Scientific Instruments **61**, 965 (1990).